Spectroscopic Characterization of an Engineered Purple Cu_A Center in Azurin

Michael T. Hay,[†] Marjorie C. Ang,[†] Daniel R. Gamelin,[‡] Edward I. Solomon,[‡] William E. Antholine,[∥] Martina Ralle,[⊥] Ninian J. Blackburn,[⊥] Priscilla D. Massey,[†] Xiaotang Wang,[†] Angela H. Kwon,[†] and Yi Lu*[,†]

Department of Chemistry, University of Illinois at Urbana−Champaign, Urbana, Illinois 61801, Department of Chemistry, Stanford University, Stanford, California 94305, National Biomedical ESR Center, Medical College of Wisconsin, Milwaukee, Wisconsin 53226, and Department of Chemistry, Biochemistry, and Molecular Biology, Oregon Graduate Institute of Science and Technology, P.O. Box 91000, Portland, Oregon 97291

Received September 25, 1997

Spectroscopic characterization of a purple Cu_A center engineered into the blue copper protein azurin from *Pseudomonas aeruginosa* (called purple Cu_A azurin hereafter) is presented. Both electrospray mass spectrometry and copper analysis indicated the protein binds two copper ions per protein. The electronic absorption (UV−vis), magnetic circular dichroism (MCD), multifrequency electron paramagnetic resonance (EPR), and X-ray absorption (XAS) spectra of the purple Cu_A azurin are strikingly similar to other native or engineered Cu_A centers, indicating that they all share similar geometric and electronic structures. It has the characteristic UV−vis absorption spectrum of a Cu_A center with absorption bands at 485 ($\epsilon = 3730$), 530 ($\epsilon = 3370$), 360 ($\epsilon = 550$), and 770 nm ($\epsilon = 1640$ M^{-1} cm^{-1}). The MCD spectrum of purple Cu_A azurin is dominated by a pair of intense, oppositely-signed features occurring at 480 nm ($\Delta\epsilon = -118$ deg M^{-1} cm^{-1} T^{-1}) and 530 nm ($\Delta\epsilon = 155$ deg M^{-1} cm^{-1} T^{-1}) and a negative feature occurring at 810 nm ($\Delta\epsilon = -52$ deg M^{-1} cm^{-1} T^{-1}). Multifrequency EPR spectra show a well-resolved seven-line hyperfine structure in the $g_{\|}$ region, typical of a delocalized mixed-valence [Cu(1.5)···Cu(1.5)] binuclear center. Compared with other delocalized mixed-valence Cu_A centers, this purple Cu_A azurin has a relatively high energy near-IR Cu−Cu $\sigma \rightarrow \sigma^*$ absorption at 770 nm, the largest $A_{\|}$ at 55 G, and the shortest Cu−Cu distance at 2.39 Å. These results may reflect a more sterically compressed Cu_A center in azurin, perhaps as the result of forcing the normally mononuclear blue copper center in azurin to accept a binuclear Cu_A center, and are consistent with the general trend between the near-IR Cu−Cu $\sigma \rightarrow \sigma^*$ absorption and the degree of $Cu_2(SR)_2$ core contraction.

Introduction

Purple Cu_A centers are a new class of copper centers in biological systems.[1−4] They are found in cytochrome *c* oxidase (COX),[5−9] a terminal oxidase in the respiratory chain of eukaryotic mitochondria and some aerobic bacteria, and nitrous oxide reductase (N_2OR),[10,11] an enzyme responsible for the reduction of N_2O in denitrifying bacteria. The purple Cu_A center is involved in biological electron transfer (ET)[5−9,12] and is believed to be responsible for ET from cytochrome *c* to heme *a* in COX and from cytochrome *c* to the catalytic Cu_Z center in N_2OR. The similarity between the Cu_A centers in COX and in N_2OR was established by both MCD[13−16] and multifrequency EPR studies.[17−20] These and other spectroscopic studies[21−30] have shown that the purple Cu_A center is different from the established three types of copper centers[31,32] found in biological

[†] University of Illinois at Urbana−Champaign.
[‡] Stanford University.
[∥] National Biomedical ESR Center, Medical College of Wisconsin.
[⊥] Oregon Graduate Institute of Science and Technology.

(1) Malmström, B. G.; Aasa, R. *FEBS Lett.* **1993**, *325*, 49−52.
(2) Lappalainen, P.; Saraste, M. *Biochim. Biophys. Acta Bioenerg.* **1994**, *1187*, 222−225.
(3) Dennison, C.; Canters, G. W. *Rec. Trav. Chim. Pays- Bas* **1996**, *115*, 345−351.
(4) Beinert, H. *Eur. J. Biochem.* **1997**, *245*, 521−532.
(5) Saraste, M. *Q. Rev. Biophys.* **1990**, *23*, 331−366.
(6) Malmström, B. G. *Chem. Rev.* **1990**, *90*, 1247−1260.
(7) Babcock, G. T.; Wikstrom, M. *Nature* **1992**, *356*, 301−309.
(8) Musser, S. M.; Stowell, M. H. B.; Chan, S. I. *FEBS Lett.* **1993**, *327*, 131−136.
(9) García-Horsman, J. A.; Barquera, B.; Rumbley, J.; Ma, J.; Gennis, R. B. *J. Bacteriol.* **1994**, *176*, 5587−5600.
(10) Kroneck, P. M. H.; Riester, J.; Zumft, W. G.; Antholine, W. E. *Biol. Met.* **1990**, *3*, 103−109.
(11) Zumft, W. G.; Kroneck, P. M. H. *Adv. Inorg. Biochem.* **1996**, *11*, 193−221.
(12) Ramirez, B. E.; Malmström, B. G.; Winkler, J. R.; Gray, H. B. *Proc. Natl. Acad. Sci. U.S.A.* **1995**, *92*, 11949−11951.
(13) Greenwood, C.; Hill, B. C.; Barber, D.; Eglinton, D. G.; Thomson, A. J. *Biochem. J.* **1983**, *215*, 303−316.
(14) Dooley, D. M.; McGuirl, M. A.; Rosenzweig, A. C.; Landin, J. A.; Scott, R. A.; Zumft, W. G.; Devlin, F.; Stephens, P. J. *Inorg. Chem.* **1991**, *30*, 3006−3011.
(15) Thomson, A. J.; Greenwood, C.; Peterson, J.; Barrett, C. P. *J. Inorg. Biochem.* **1986**, *28*, 195−205.
(16) Farrar, J. A.; Thomson, A. J.; Cheesman, M. R.; Dooley, D. M.; Zumft, W. G. *FEBS Lett.* **1991**, *294*, 11−15.
(17) Riester, J.; Zumft, W. G.; Kroneck, P. M. H. *Eur. J. Biochem.* **1989**, *178*, 751−762.
(18) Antholine, W. E.; Kastrau, D. H. W.; Steffens, G. C. M.; Buse, G.; Zumft, W. G.; Kroneck, P. M. H. *Eur. J. Biochem.* **1992**, *209*, 875−881.
(19) Kroneck, P. M. H.; Antholine, W. E.; Riester, J.; Zumft, W. G. *FEBS Lett.* **1988**, *242*, 70−74.
(20) Kroneck, P. M. H.; Antholine, W. E.; Kastrau, D. H. W.; Buse, G.; Steffens, G. C. M.; Zumft, W. G. *FEBS Lett.* **1990**, *268*, 274−276.
(21) Beinert, H.; Griffiths, D. E.; Wharton, D. C.; Sands, R. H. *J. Biol. Chem.* **1962**, *237*, 2337−2346.
(22) Peisach, J.; Blumberg, W. E. *Arch. Biochem. Biophys.* **1974**, *165*, 691−708.
(23) Mims, W. B.; Peisach, J.; Shaw, R. W.; Beinert, H. *J. Biol. Chem.* **1980**, *255*, 6843−6846.

S0020-1669(97)01232-9 CCC: $15.00
Published on Web 01/01/1998

systems. In particular, the observation of a seven-line hyperfine splitting in the multifrequency EPR studies of the Cu_A center in both COX and N_2OR by Antholine, Kroneck, Zumft, and co-workers provided strong support for the existence of a mixed-valent [Cu(1.5)···Cu(1.5)] center.[17−20]

More thorough study of the purple Cu_A center was aided by the availability of water-soluble proteins containing only a single Cu_A center, such as N_2OR V (an N_2OR mutant protein that contains only the Cu_A center),[17] the CyoA construct (a soluble domain of *Escherichia coli* quinol oxidase in which a Cu_A center has been introduced),[33,34] and soluble domains of subunit II of *Paracoccus denitrificans*,[35] *Bacillus subtilis*,[36] *and Thermus thermophilus*[37] COX expressed in *E. coli*. It is now known that all of the purple Cu_A centers display an intense purple color with strong electronic absorption bands around 480 and 530 nm[17,33,35−37] and a characteristic resonance Raman Cu−S stretching frequency around 340 cm^{-1}.[38−41] These and other spectroscopic studies on water-soluble proteins containing the purple Cu_A center by EPR,[36,42−45] MCD,[45,46] XAS,[47−49] and paramagnetic NMR[50−52] of COX and N_2OR have established the existence of the mixed-valence [Cu(1.5)···Cu(1.5)] binuclear center in the Cu_A sites. Amino acid sequence analysis and site-directed mutagenesis have identified the conserved amino acids (two cysteines, two histidines, and one methionine) as potential ligands to the copper center.[34,53] Three crystal structures of proteins containing the purple Cu_A center at 2.8 Å (COX from bovine heart[54,55] and from *P. denitrificans*[56]) and 2.3 Å (CyoA construct[57]) have been published. They have confirmed the protein engineering and spectroscopic studies, and established the mixed-valence binuclear Cu_2S_2 structural core (see Figure 1).[4,58−60] Molecular orbital calculations and spectroscopic assignments have also been carried out.[42,44,45,61]

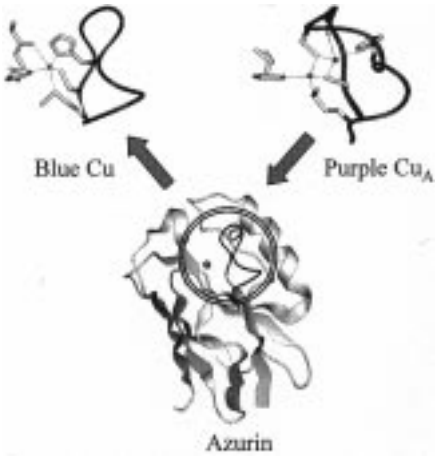

Figure 1. Structure of the blue copper azurin from *P. aeruginosa*. The loop containing the ligands to the blue copper center (highlighted in the circle) has been replaced by a ligand loop sequence similar to that of the purple Cu_A center in COX from *P. denitrificans* (see Table 1).

Azurin is a classic blue (type 1) copper protein.[62] It has an intense blue color with a strong absorption around 625 nm[63] and a characteristic resonance Raman Cu−S stretching frequency around 408 cm^{-1}.[64] Extensive spectroscopic,[65] X-ray crystallographic[66−68] and protein engineering studies,[69−72] as well as electronic structure calculations,[73] have made azurin one

(24) Brudvig, G. W.; Blair, D. F.; Chan, S. I. *J. Biol. Chem.* **1984**, *259*, 11001−11009.
(25) Fan, C.; Bank, J. F.; Dorr, R. G.; Scholes, C. P. *J. Biol. Chem.* **1988**, *263*, 3588−3591.
(26) Scott, R. A. *Annu. Rev. Biophys. Biophys. Chem.* **1989**, *18*, 137−158.
(27) Hulse, C. L.; Averill, B. A. *Biochem. Biophys. Res. Commun.* **1990**, *166*, 729−735.
(28) Gurbiel, R. J.; Fann, Y. C.; Surerus, K. K.; Werst, M. M.; Musser, S. M.; Doan, P. E.; Chan, S. I.; Fee, J. A.; Hoffman, B. M. *J. Am. Chem. Soc.* **1993**, *115*, 10888−10894.
(29) Hansen, A. P.; Britt, R. D.; Klein, M. P.; Bender, C. J.; Babcock, G. T. *Biochemistry* **1993**, *32*, 13718−13724.
(30) Henkel, G.; Müller, A.; Weissgräber, S.; Buse, G.; Soulimane, T.; Steffens, G. C. M.; Nolting, H.-F. *Angew. Chem., Int. Ed. Engl.* **1995**, *34*, 1488−1492.
(31) Fee, J. A. *Struct. Bonding (Berlin)* **1975**, *23*, 1−60.
(32) Malkin, R.; Malmström, B. G. *Adv. Enzymol.* **1970**, *33*, 177−244.
(33) van der Oost, J.; Lappalainen, P.; Musacchio, A.; Warne, A.; Lemieux, L.; Rumbley, J.; Gennis, R. B.; Aasa, R.; Pascher, T.; Malmström, B. G.; Saraste, M. *EMBO J.* **1992**, *11*, 3209−3217.
(34) Kelly, M.; Lappalainen, P.; Talbo, G.; Haltia, T.; van der Oost, J.; Saraste, M. *J. Biol. Chem.* **1993**, *268*, 16781−16787.
(35) Lappalainen, P.; Aasa, R.; Malmström, B. G.; Saraste, M. *J. Biol. Chem.* **1993**, *268*, 26416−26421.
(36) von Wachenfeldt, C.; de Vries, S.; van der Oost, J. *FEBS Lett.* **1994**, *340*, 109−113.
(37) Slutter, C. E.; Sanders, D.; Wittung, P.; Malmström, B. G.; Aasa, R.; Richards, J. H.; Gray, H. B.; Fee, J. A. *Biochemistry* **1996**, *35*, 3387−3395.
(38) Andrew, C. R.; Lappalainen, P.; Saraste, M.; Hay, M. T.; Lu, Y.; Dennison, C.; Canters, G. W.; Fee, J. A.; Slutter, C. E.; Nakamura, N.; Sanders-Loehr, J. *J. Am. Chem. Soc.* **1995**, *117*, 10759−10760.
(39) Andrew, C. R.; Han, J.; de Vries, S.; van der Oost, J.; Averill, B. A.; Loehr, T. M.; Sanders-Loehr, J. *J. Am. Chem. Soc.* **1994**, *116*, 10805−10806.
(40) Andrew, C. R.; Fraczkiewicz, R.; Czernuszewicz, R. S.; Lappalainen, P.; Saraste, M.; Sanders-Loehr, J. *J. Am. Chem. Soc.* **1996**, *118*, 10436−10445.
(41) Andrew, C. R.; Sanders-Loehr, J. *Acc. Chem. Res.* **1996**, *29*, 365−372.
(42) Neese, F.; Zumft, W. G.; Antholine, W. E.; Kroneck, P. M. H. *J. Am. Chem. Soc.* **1996**, *118*, 8692−8699.
(43) Fee, J. A.; Sanders, D.; Slutter, C. E.; Doan, P. E.; Aasa, R.; Karpefors, M.; Vänngård, T. *Biochem. Biophys. Res. Commun.* **1995**, *212*, 77−83.
(44) Karpefors, M.; Slutter, C. E.; Fee, J. A.; Aasa, R.; Kallebring, B.; Larsson, S.; Vänngård, T. *Biophys. J.* **1996**, *71*, 2823−2829.
(45) Farrar, J. A.; Neese, F.; Lappalainen, P.; Kroneck, P. M. H.; Saraste, M.; Zumft, W. G.; Thomson, A. J. *J. Am. Chem. Soc.* **1996**, *118*, 11501−11514.
(46) Farrar, J. A.; Lappalainen, P.; Zumft, W. G.; Saraste, M.; Thomson, A. J. *Eur. J. Biochem.* **1995**, *232*, 294−303.
(47) Blackburn, N. J.; Barr, M. E.; Woodruff, W. H.; van der Oost, J.; de Vries, S. *Biochemistry* **1994**, *33*, 10401−10407.
(48) Williams, K. R.; Gamelin, D. R.; LaCroix, L. B.; Houser, R. P.; Tolman, W. B.; Mulder, T. C.; de Vries, S.; Hedman, B.; Hodgson, K. O.; Solomon, E. I. *J. Am. Chem. Soc.* **1997**, *119*, 613−614.
(49) Blackburn, N. J.; de Vries, S.; Barr, M. E.; Houser, R. P.; Tolman, W. B.; Sanders, D.; Fee, J. A. *J. Am. Chem. Soc.* **1997**, *119*, 6135−6143.
(50) Dennison, C.; Berg, A.; de Vries, S.; Canters, G. W. *FEBS Lett.* **1996**, *394*, 340−344.
(51) Bertini, I.; Bren, K. L.; Clemente, A.; Fee, J. A.; Gray, H. B.; Luchinat, C.; Malmström, B. G.; Richards, J. H.; Sanders, D.; Slutter, C. E. *J. Am. Chem. Soc.* **1996**, *118*, 11658−11659.
(52) Dennison, C.; Berg, A.; Canters, G. W. *Biochemistry* **1997**, *36*, 3262−3269.
(53) Speno, H.; Taheri, M. R.; Sieburth, D.; Martin, C. T. *J. Biol. Chem.* **1995**, *270*, 25363−25369.
(54) Tsukihara, T.; Aoyama, H.; Yamashita, E.; Tomizaki, T.; Yamaguchi, H.; Shinzawa-Itoh, K.; Nakashima, R.; Yaono, R.; Yoshikawa, S. *Science* **1995**, *269*, 1069−1074.
(55) Tsukihara, T.; Aoyama, H.; Yamashita, E.; Tomizaki, T.; Yamaguchi, H.; Shinzawa-Itoh, K.; Nakashima, R.; Yaono, R.; Yoshikawa, S. *Science* **1996**, *272*, 1136−1144.
(56) Iwata, S.; Ostermeier, C.; Ludwig, B.; Michel, H. *Nature* **1995**, *376*, 660−669.
(57) Wilmanns, M.; Lappalainen, P.; Kelly, M.; Sauer-Eriksson, E.; Saraste, M. *Proc. Natl. Acad. Sci. U.S.A.* **1995**, *92*, 11955−11959.
(58) Gennis, R.; Ferguson-Miller, S. *Science* **1995**, *269*, 1063−1064.
(59) Scott, R. A. *Structure* **1995**, *3*, 981−986.
(60) Kadenbach, B. *Angew. Chem., Int. Ed. Engl.* **1995**, *34*, 2635−2637.
(61) Larsson, S.; Källebring, B.; Wittung, P.; Malmström, B. G. *Proc. Natl. Acad. Sci. U.S.A.* **1995**, *92*, 7167−7171.
(62) Gray, H. B.; Solomon, E. I. In *Copper Proteins*; Spiro, T. G., Ed.; Wiley: New York, 1981; pp 1−39.
(63) McMillin, D. R. *Bioinorg. Chem.* **1978**, *8*, 179−184.

Table 1. DNA Primers and Amino Acid Sequences of the Ligand Loop

PstI-21

PstI

5'- CGT AAG CTG GCT GCA GTG TCT

Bak-72

Cys Ser Glu Leu Cys Gly Ile Asn His Ala Leu Met KpnI

5'-GAA CAG TAC ATG TTC TTC TGC TCC GAA CTG TGC GGT ATC AAC CAC GCT CTG ATG AAA GGT ACC CTG ACT CTG

CTT GTC ATG TAC AAG AAG ACG AGG CTT GAC ACG CCA TAG TTG GTG CGA GAC TAC TTT CCA TGG GAC TGA GAC-5'

of the best understood copper centers in biological systems. As shown in Figure 1, the blue copper is in a trigonal-pyramidal center with one cysteine and two histidines in the trigonal plane, and one methionine and one long nonbonded carbonyl oxygen from the peptide backbone in the axial positions. Despite a poor amino acid sequence homology, the blue copper and purple Cu_A centers share strong structural homology of the Greek key β-barrel fold as indicated by amino acid sequence alignment.[5,74] This similarity has been confirmed by the availability of the crystal structures of proteins containing the purple Cu_A sites.[54−56] The major difference resides in the ligand loop shown in Figure 1. Therefore we have taken advantage of this difference and converted the blue copper protein azurin from *Pseudomonas aeruginosa* into a purple copper center by replacing the ligand loop of azurin with that of the Cu_A center in COX from *P. denitrificans*.[75] Using the same approach, Canters and co-workers have introduced the purple Cu_A center into another blue copper protein amicyanin from *Thiobacillus versutus*.[50,76] Metal ion substitution study by Hg(II) and Ag(I) on the engineered purple Cu_A azurin showed that Hg(II) replaces Cu(II) preferentially and $Hg^{II}Ag^{I}$ is the most stable derivative, suggesting that the purple Cu_A center is built so that a net +4-charged [M(II)···M(II)] in the binding site is less favored than the +3-charged [M(II)···M(I)] (or [M(1.5)···M(1.5)]) derivative.[77] The ability to incorporate either a blue copper or a purple Cu_A center into the same protein framework facilitates comparison of the structural properties of these two important classes of copper centers. In addition, since both copper centers are involved in biological electron transfer,[12,78−80] studies of both centers under the same protein framework will offer insight into the contribution of the different metal-binding sites in biological electron transfer.

Here we present spectroscopic studies of this engineered Cu_A center in azurin. Results from UV−vis, ES-MS, MCD, multifrequency EPR, and XAS of the engineered purple copper azurin show striking similarity to the Cu_A sites in COX and N_2OR. When compared to the other delocalized mixed-valence Cu_A centers studied to date, the purple Cu_A azurin has one of the highest-energy near-IR Cu−Cu $\sigma \rightarrow \sigma^*$ absorption features at 770 nm, the largest $A_{\|}$ at 55 G, and the shortest Cu−Cu distance at 2.39 Å. These results will be presented, together with a discussion of their relationship with the structures of both blue and purple Cu_A centers.

Experimental Section

Materials and Methods. Copper(II) sulfate, 2-propanol, acetonitrile, 30% hydrogen peroxide, hydrochloric acid, 88% formic acid, ammonium hydroxide, sodium hydroxide, sodium chloride, and ammonium acetate were all purchased from Fischer Scientific (Pittsburgh, PA). Copper(II) chloride was purchased from Aldrich (Milwaukee, WI), and $Cu^{I}(CH_3CN)_4BF_4$ was a gift from Professor John Shapley at the University of Illinois. The Bradford protein assay dye solution was purchased from Bio-Rad (Hercules, CA). All chemicals were used without further purification. Ultrafiltration stirred cells and centricon-10 concentrators were purchased from Amicon, Inc. (Beverly, MA). SP Sepharose FF media, prepacked disposable PD-10 gel filtration columns, and a Resource Q anion-exchange column were purchased from Pharmacia Biotech. Low-pressure protein purification was performed on a GradiFrac system from Pharmacia Biotech. High-pressure protein purification was performed on a BioCad Sprint perfusion chromatography system from PerSeptive Biosystems.

Construction of the Purple Cu_A Azurin by Loop-directed Mutagenesis. The mutant DNA was constructed[75] on a recombinant azurin gene from *P. aeruginosa*[81] using a PCR mutagenesis method.[82] Two primers were used in PCR mutagenesis (see Table 1). The forward primer (For-21) covers the azurin gene where a unique Pst I restriction site is located. The backward primer (Bak-72) contains the new loop sequence and a unique Kpn I site. The PCR-amplified fragment containing the azurin gene with the new loop sequence was digested with Pst I and Kpn I restriction enzymes. This fragment can then replace the corresponding Pst I-Kpn I fragment in the wild-type azurin by molecular cloning. The mutation was confirmed first by a restriction digest because the use of Bak-72 primer also eliminated a Xma I site. The mutant DNA sequence was further verified by the dideoxyribonucleotide method using an ABI 373 automated sequencer in the Biotechnology Center at the University of Illinois.

Expression and Purification of the Purple Cu_A Azurin. The apoprotein was over-expressed in *E. coli* as described previously[81,83] with minor modifications. Briefly, after acidification of the protein extract with 1/10 volume of 0.5 M sodium acetate (pH 4.1) solution,

(64) Andrew, C. R.; Yeom, H.; Valentine, J. S.; Karlsson, B. G.; Bonander, N.; van Pouderoyen, G.; Canters, G. W.; Loehr, T. M.; Sanders-Loehr, J. *J. Am. Chem. Soc.* **1994**, *116*, 11489−11498.
(65) Solomon, E. I.; Hare, J. W.; Gray, H. B. *Proc. Natl. Acad. Sci. U.S.A.* **1976**, *73*, 1389−1393.
(66) Adman, E. T. *Adv. Protein Chem.* **1991**, *42*, 145−197.
(67) Baker, E. N. *J. Mol. Biol.* **1988**, *203*, 1071−1095.
(68) Nar, H.; Messerschmidt, A.; Huber, R.; van der Kamp, M.; Canters, G. W. *J. Mol. Biol.* **1991**, *221*, 765−772.
(69) Kroes, S. J.; Hoitink, C. W. G.; Andrew, C. R.; Ai, J.; Sanders-Loehr, J.; Messerschmidt, A.; Hagen, W. R.; Canters, G. W. *Eur. J. Biochem.* **1996**, *240*, 342−351.
(70) van Pouderoyen, G.; Andrew, C. R.; Loehr, T. M.; Sanders-Loehr, J.; Mazumdar, S.; Hill, H. A. O.; Canters, G. W. *Biochemistry* **1996**, *35*, 1397−1407.
(71) Karlsson, B. G.; Nordling, M.; Pascher, T.; Tsai, L.-C.; Sjolin, L.; Lundberg, L. G. *Protein Eng.* **1991**, *4*, 343−349.
(72) Pascher, T.; Bergström, J.; Malmström, B. G.; Vänngård, T.; Lundberg, L. G. *FEBS Lett.* **1989**, *258*, 266−268.
(73) Solomon, E. I.; Baldwin, M. J.; Lowery, M. D. *Chem. Rev.* **1992**, *92*, 521−542.
(74) Steffens, G. J.; Buse, G. *Hoppe-Seyler's Z. Physiol. Chem.* **1979**, *360*, 613−619.
(75) Hay, M.; Richards, J. H.; Lu, Y. *Proc. Natl. Acad. Sci. U.S.A.* **1996**, *93*, 461−464.
(76) Dennison, C.; Vijgenboom, E.; de Vries, S.; van der Oost, J.; Canters, G. W. *FEBS Lett.* **1995**, *365*, 92−94.
(77) Hay, M. T.; Milberg, R. M.; Lu, Y. *J. Am. Chem. Soc.* **1996**, *118*, 11976−11977.
(78) Farver, O.; Pecht, I. In *Copper Proteins*; Spiro, T. G., Ed.; Wiley: New York, 1981; pp 151−192.
(79) Sykes, A. G. *Chem. Soc. Rev.* **1985**, *14*, 283−315.
(80) Gray, H. B. *Chem. Soc. Rev.* **1986**, *15*, 17−30.
(81) Chang, T. K.; Iverson, S. A.; Rodrigues, C. G.; Kiser, C. N.; Lew, A. Y. C.; Germanas, J. P.; Richards, J. H. *Proc. Natl. Acad. Sci. U.S.A.* **1991**, *88*, 1325−1329.
(82) *PCR Protocol*; Innis, M. A., Gelfand, D. H., Sninsky, J. J., White, T. J., Eds.; Academic Press: San Diego, CA, 1990; pp 177−183.
(83) Mizoguchi, T. J.; Di Bilio, A. J.; Gray, H. B.; Richards, J. H. *J. Am. Chem. Soc.* **1992**, *114*, 10076−10078.

the clear supernatant was purified on a SP Sepharose FF column using a GradiFrac system and a pH gradient from 100% 50 mM ammonium acetate buffer pH 4.1 to 100% 50 mM ammonium acetate buffer pH 5.8. Apo-Cu_A-azurin was eluted at pH 5.2. After purification, the apoprotein was stored in a Schlenk flask under an atmosphere of argon at 4 °C. The protein is stable up to 3 months under this condition. Holoprotein can be prepared either by addition of $CuSO_4$ alone or by addition of approximately 1 equiv of $Cu(CH_3CN)_4BF_4$ in a 50/50 mixture of buffer/acetonitrile first, followed by addition of another 1 equiv of $CuSO_4$. The buffer of the holoprotein was exchanged to 1 mM bis-tris propane (pH 7.0) using a PD-10 gel filtration column. The holoprotein was then purified to homogeneity through a Resource Q column, on a BioCad/Sprint system using a salt gradient from 5 mM bis-tris propane (pH 7.0) to a buffer containing 5 mM bis-tris propane (pH 7.0) and 20 mM NaCl. Fractions were immediately diluted with 200 mM ammonium acetate (pH 5.1) in order to store the purified protein at a stable pH. The purple holoprotein was concentrated to an appropriate volume using a stirred-cell ultrafiltration apparatus. The buffer was exchanged to 50 mM ammonium acetate (pH 5.1) using a PD-10 gel filtration column. The purified holoprotein was then flashed frozen in liquid nitrogen and stored under liquid nitrogen or in a −80 °C freezer for several months, with little detectable decomposition.

Protein Analyses. The protein concentration ($\epsilon_{280} = 7830\ M^{-1}\ cm^{-1}$ for holoprotein) was determined by quantitative amino acid analyses, by a Bradford assay method using a dye solution from Bio-Rad and bovine serum albumin as a standard or spectrophotometry at 205 nm.[84] The extinction coefficient at 485 nm ($\epsilon_{485\ nm} = 3730\ M^{-1}\ cm^{-1}$) was estimated by two methods: (a) from $\epsilon_{280\ nm} = 7830\ M^{-1}\ cm^{-1}$ for a homogeneous holoprotein sample and the ratio of A_{280}/A_{485}; (b) from a careful titration of apoprotein with $CuSO_4$. Upon saturation of the visible spectrum of the Cu_A azurin, the volume and concentration of the $CuSO_4$ consumed was used to determine the concentration of holoprotein, assuming two copper ions per protein. The extinction coefficient at 485 nm was then calculated on the basis of the absorption at 485 nm and the concentration of the holoprotein. The above methods of estimation agree with each other within experimental error.

Copper Analyses. The copper content was analyzed by integrating the Cu(II) EPR spectra of denatured and fully oxidized holoprotein and comparing those with standard $CuCl_2$ solutions.[37] The protein concentration was estimated using the $\epsilon_{485\ nm} = 3730\ M^{-1}\ cm^{-1}$. Aliquots of holoprotein (100 μL) were dissolved in denaturing solution (60% HCOOH, 30% 2-propanol, and 10% water) (390 μL) and 30% H_2O_2 (10 μL). The X-band EPR was measured at 77 K, and the total spin due to copper (II) was integrated. The integrated spin was then calibrated against a standard curve from the integrated $CuCl_2$ spins of known concentration to give the number of copper atoms per protein. The Cu/protein ratio was determined to be 1.8, based on the average of three trials.

Electrospray Mass Spectrometry (ES-MS). The ES-MS data were acquired in the continuum mode using a Quattro instrument capable of unit mass resolution below 2000 molecular weight (50% valley definition). The mass scale was calibrated with CsI. The electrospray ionization was performed with a 100% water flow system at 15 μL/min into the ion source, and the sample was in ammonium acetate (pH 5.1) buffer. No counterions were introduced into the mass spectrometer's analyzer. Multiple charged ions (typically 6, 7, and 8 positive charged species) were observed under the condition employed. The multiple charged data were then transformed into the singly charged spectra presented in the paper.

Electronic Absorption (UV−Vis). The UV−vis spectra were recorded on a Cary 3E spectrophotometer (Varian, TX) at ambient temperature.

Magnetic Circular Dichroism (MCD). The 4.2 K 7 T MCD spectra of the purple Cu_A azurin were collected using Jasco J500 (UV/vis/near-IR, S1 and S20 PMT detection) and J200 (near-IR, InSb detection) CD spectropolarimeters with sample compartments modified to accommodate Oxford Instruments SM4-7T cryogenic superconducting magneto-optical dewars. For MCD measurements, 1 mM samples of purple Cu_A azurin in 50 mM ammonium acetate buffer (pH 5.1) were diluted with glycerol-d_3 (66% v/v) and injected into a sample cell comprised of two quartz disks separated by a Viton O-ring spacer. Negligible depolarization (<5%) by the sample at liquid helium temperatures was confirmed by monitoring the CD signal of a nickel (+)-tartrate solution placed before and after the sample compartment. The MCD $\Delta\epsilon$ values reported are obtained by scaling the low-temperature absorption and MCD intensities measured on the same sample by $\epsilon_{485\ nm} = 3730\ M^{-1}\ cm^{-1}$. All MCD intensities are reported on a per tesla scale in the linear (low-field) region of the $S = {}^1/_2$ saturation curve.

Multifrequency Electron Paramagnetic Resonance (EPR). X-band spectra were obtained on a Varian Century Series spectrometer (Varian, Palo Alto, CA). S-band (3.4 GHz) and C-band (4.5 GHz) spectra were obtained with an S-band bridge or a C-band bridge, loop-gap resonators, and supporting equipment developed at the National Biomedical ESR Center.[85] Temperatures were maintained with a helium-flow system (Air-Products, Allentown, PA). The first harmonics of spectra were obtained using the program SUMSPC92, which is available upon request from the ESR Center in Milwaukee, WI.

X-ray absorption (XAS). XAS data were collected at the Stanford Synchrotron Radiation Laboratory (SSRL) on beam line 7.3, with beam energy of 3 GeV and maximum stored beam currents between 100 and 50 mA. The Si(220) monochromator was detuned 50% to reject harmonics. Protein samples were measured as frozen aqueous glasses in 20% glycerol, at a temperature of 10−20 K. The Cu K-absorption spectrum was obtained by measuring the Cu Kα fluorescence using an appropriately windowed 13-element Ge detector. To avoid detector saturation, the count rate of each detector channel was kept below 100 kHz. The count rate was controlled by adjusting the hutch entrance slits or by moving the detector in or out from the cryostat windows. Under these conditions, no dead-time correction was necessary. The summed data for each detector were inspected, and only those channels that gave high-quality backgrounds free from drop outs, glitches, or ice diffraction peaks were included in the final average. Seven scans were included in the averaged spectra. The averaged data were background subtracted and normalized to the smoothly varying background atomic absorption using the EXAFS data reduction package EXAFSPAK.[86] The experimental energy threshold ($k = 0$) was chosen as 8985 eV. Energy calibration was achieved by reference to the first inflection point of a copper foil (8980.3 eV) placed between the second and third ion chambers. In any series of scans, the measured energy of the first inflection of the copper foil spectrum varied by less than 1 eV. Averaged EXAFS data were referenced to the copper calibration of the first scan of a series, since the energy drift in any series of scans was too small to perturb the EXAFS oscillations. However, this drift led to broadening of edge features when a series of scans was averaged. Consequently, for edge analysis a single scan was used. Data analysis was carried out by least-squares curve fitting utilizing full curved-wave calculations as formulated by the SRS library program EXCURV,[87−90] using methodology described in detail previously.[91−93] The parameters refined in the fit were as follows: E_o, the photoelectron energy threshold; R_i the distance from Cu to atom i; $2\sigma^2_i$ the Debye−Waller term for atom i. Coordination numbers were fixed at the values determined from the crystal structures.

The quality of the fits was determined using a least-squares fitting parameter, F, defined as

(84) Stoscheck, C. M. *Methods Enzymol.* **1990**, *182*, 50−67.

(85) Froncisz, W.; Hyde, J. S. *J. Magn. Reson.* **1982**, *47*, 515−521.
(86) George, G. N. *EXAFSPAK*; George, G. N., Ed.; Stanford Synchrotron Radiation Laboratory: Stanford, CA, 1990.
(87) Binsted, N.; Gurman, S. J.; Campbell, J. W. *Daresbury Laboratory EXCURV88 Program*; Daresburg Laboratory: Daresburg, U.K., 1988.
(88) Gurman, S. J. In *Synchrotron Radiation and Biophysics*; Hasnain, S. S., Ed.; Ellis Horwood Ltd.: Chichester, U.K., 1989; pp 9−42.
(89) Gurman, S. J.; Binsted, N.; Ross, I. *J. Phys. C* **1984**, *17*, 143−151.
(90) Gurman, S. J.; Binsted, N.; Ross, I. *J. Phys. C* **1986**, *19*, 1845−1861.
(91) Strange, R. W.; Blackburn, N. J.; Knowles, P. F.; Hasnain, S. S. *J. Am. Chem. Soc.* **1987**, *109*, 7157−7162.
(92) Blackburn, N. J.; Hasnain, S. S.; Pettingill, T. M.; Strange, R. W. *J. Biol. Chem.* **1991**, *266*, 23120−23127.
(93) Sanyal, I.; Karlin, K. D.; Strange, R. W.; Blackburn, N. J. *J. Am. Chem. Soc.* **1993**, *115*, 11259−11270.

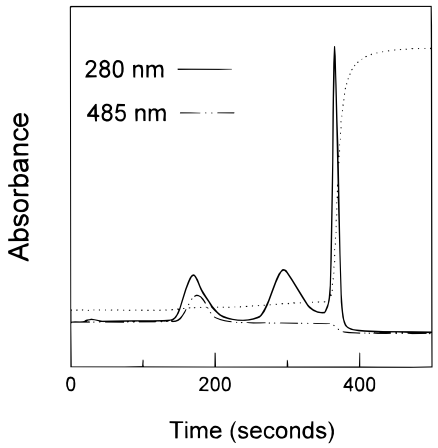

Figure 2. Chromatogram of HPLC purification of the purple Cu_A azurin. The first peak exhibited both 280 nm (—) and 485 nm (—••—) absorption under a salt gradient (•••) and was collected for further study (see Experimental Section for detailed conditions).

$$F^2 = (1/N)\sum k^6(\chi_i^{\text{theor}} - \chi_i^{\text{exp}})^2$$

referred to as the fit index, where N is the number of points in the spectrum.

Results and Discussion

Construction, Expression, and Purification of Purple Cu_A Azurin. The purple Cu_A azurin was constructed and expressed in *E. coli* as described previously.[75] The holoprotein was purified to homogeneity by HPLC (Figure 2). The peak displaying both the 280- and 485-nm absorption bands was collected. Its homogeneity was confirmed by either SDS-PAGE (data not shown) or by ES-MS (Figure 3). The holoprotein displayed one ES-MS peak (*m*/*e*) at 14 295, consistent with the calculated molecular weight of apoprotein (14 168) plus two copper ions (127). Upon addition of increasing amounts of formic acid, the intensity of the parent peak decreases and a new peak, one with the molecular weight of apoprotein (14 168), was detected. The ES-MS results indicate that the protein sample is homogeneous, and contains two copper ions in the resting form. Similar results have been obtained on other Cu_A-containing proteins.[36] Copper analyses by EPR spectral integration of denatured holo-purple Cu_A azurin (see Experimental Section) confirmed that the Cu/protein ratio is around 2.0. We chose EPR spectral integration over other copper analysis methods such as induction coupled plasma or bathocupreine sulfonate because Slutter *et al.*[37] have shown that, among those copper ion analysis methods, the EPR spectral integration method gave more precise measurements of total copper contents in the Cu_A domain of *T. thermophilus*.

Spectroscopic Characterization. UV−Vis Absorption and MCD. The UV−vis absorption spectra of wild-type azurin and the engineered purple Cu_A azurin are shown in Figure 4a. The absorption spectrum of wild-type azurin displays a typical blue copper spectrum with a strong absorption band at 625 nm (ϵ = 5700 M^{-1} cm^{-1}) and weaker absorption bands at 460 (ϵ = 350 M^{-1} cm^{-1}) and 765 nm (ϵ = 1200 M^{-1} cm^{-1}). The engineered purple Cu_A azurin center exhibits a dramatically different spectrum, with two strong absorption bands at 485 (ϵ = 3730 M^{-1} cm^{-1}) and 530 nm (ϵ = 3370 M^{-1} cm^{-1}), and weaker absorption bands at 360 (ϵ = 550 M^{-1} cm^{-1}) and 770 nm (ϵ = 1640 M^{-1} cm^{-1}). The purple Cu_A azurin absorption spectrum is strikingly similar to that of the native Cu_A from *P. denitrificans* as well as to other native and engineered Cu_A centers (see Table 2).

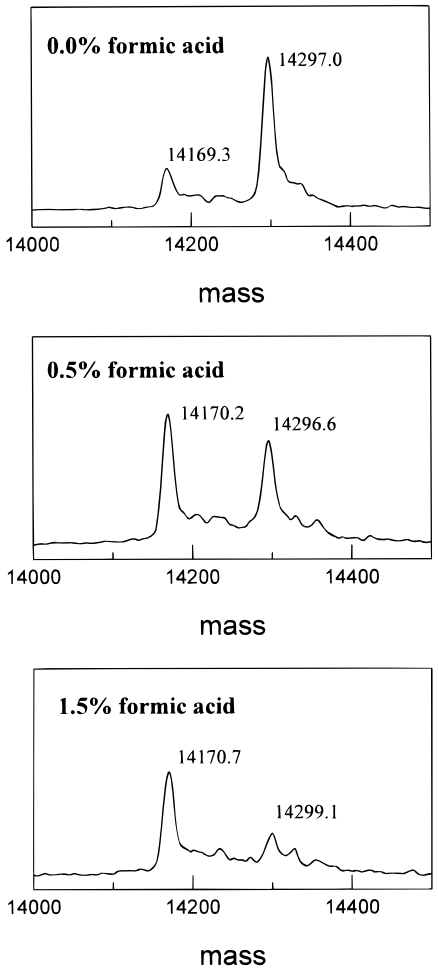

Figure 3. ES-MS spectra of the holo-purple Cu_A azurin in the presence of 0% (a), 0.5% (b), and 1.5% (c) formic acid.

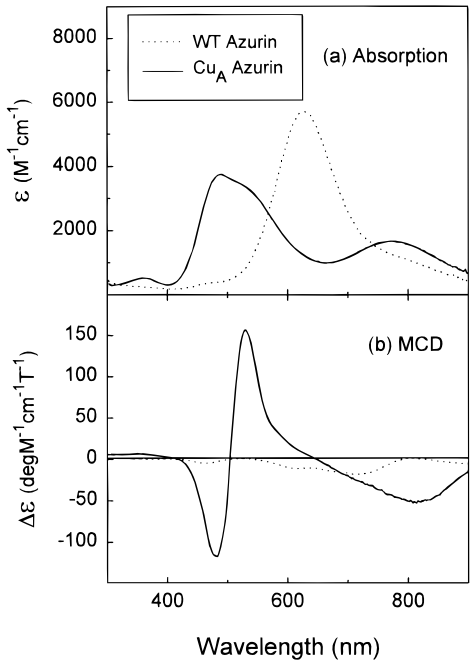

Figure 4. Room-temperature UV−vis absorption (a) and 4.2 K MCD (b) spectra of wild-type azurin from *P. aeruginosa* (•••) and the engineered purple Cu_A azurin (—).

Figure 4b shows the low-temperature MCD spectra of wild-type azurin and purple Cu_A azurin. The MCD spectrum of

Table 2. Electronic Absorption Data for Selected Purple Cu_A Centers

protein	source	abs (nm)	ref
Cu_A in N_2OR[a]	*Pseudomonas stutzeri*	350, 480, 540, 780	17
Cu_A in N_2OR[a]	*Achromobacter cycloclastes*	350, 481, 534, 780	27
Cu_A from caa_3[b]	*B. subtilis*	365, 480, 530, 790	36
Cu_A from ba_3[b]	*T. thermophilus*	360, 480, 530, 790	37
Cu_A from aa_3[b]	*P. denitrificans*	354, 485, 530, 808	35
Cu_A in azurin[c]	*P. aeruginosa*	360, 485, 530, 770	75, this work
Cu_A in amicyanin[c]	*T. versutus*	360, 483, 532, 790	76
Cu_A in CyoA[c]	*E. coli*	358, 475, 536, 765	33

[a] Native Cu_A protein. [b] Soluble Cu_A domain. [c] Engineered Cu_A protein.

purple Cu_A azurin is dominated by a pair of intense, oppositely-signed features occurring at 480 nm ($\Delta\epsilon = -118$ deg M^{-1} cm^{-1} T^{-1}) and 530 nm ($\Delta\epsilon = 155$ deg M^{-1} cm^{-1} T^{-1}), and a negative feature occurring at 810 nm ($\Delta\epsilon = -52$ deg M^{-1} $cm^{-1}T^{-1}$). An additional weaker positive feature is observed at 360 nm ($\Delta\epsilon = 6$ deg M^{-1} cm^{-1} T^{-1}), with other unresolved transitions also evident in the region between ~560 and 800 nm. As with the UV−vis absorption, the spectral features observed in the purple Cu_A azurin MCD spectrum differ dramatically from those of the wild-type azurin but are similar to those observed in wild-type Cu_A.[45,46] Most noticeably, although the UV−vis absorption intensities of the wild-type azurin and purple Cu_A azurin in the range of 450 and 650 nm are comparable, the MCD intensities observed in the purple Cu_A azurin are significantly greater than those observed in wild-type azurin.

The MCD signals shown in Figure 4b all show *C*-term temperature dependence (data not shown). Expansion of the MCD *C*-term expression shows that such intensity requires the presence of two perpendicular nonzero components (M_i) of the electric-dipole transition moment that are additionally both perpendicular to the Zeeman direction[94] (i.e., $\Delta\epsilon \propto g_z M_x M_y + g_x M_y M_z + g_y M_x M_z$). In low-symmetry protein sites such as these, all electronic states are nondegenerate and consequently at most one electric-dipole component may be nonzero for any given electronic transition. The observation of *C*-term MCD intensity therefore implicates out-of-state spin−orbit coupling in these systems. Out-of-state spin−orbit coupling allows additional components of the electric-dipole transition moment to become nonzero through mixing of the nondegenerate states and in this way provides a mechanism for low-symmetry sites to gain MCD *C*-term intensity.[95]

The two limiting cases for such out-of-state spin−orbit coupling are (a) between pairs of excited states and (b) between an excited state and the ground state.[96] MCD *C*-term intensity dominated by out-of-state spin−orbit coupling between two excited states manifests itself as a pseudo-*A*-term MCD feature, in which the MCD bands associated with the two interacting excited states have equal magnitudes but opposite signs. This is clearly the case for the two features at 485 and 530 nm in the MCD spectrum of purple Cu_A azurin, where the ratio of integrated intensities in these transitions is ~1.2:−1.0. The unusually large MCD intensities observed in purple Cu_A systems around 500 nm are therefore attributable to the presence of two intense, perpendicularly-polarized transitions at very similar energies that mix *via* spin−orbit coupling. On the basis of previous resonance Raman studies of this and related sites,[38,39,97] this pair of transitions is assigned as two S(Cys) → Cu charge-transfer (CT) transitions.

Table 3. EXAFS-Derived Cu−N(His), Cu−S(Cys), and Cu−Cu Distances for Purple Cu_A Azurin at 10 K[a]

		Cu−N(His)		Cu−S(Cys)		Cu−Cu	
	fit index	R (Å^{-1})	$2\sigma^2$ (Å^2)	R (Å^{-1})	$2\sigma^2$ (Å^2)	R (Å^{-1})	$2\sigma^2$ (Å^2)
purple Cu_A azurin	1.47	1.92	0.002	2.28	0.007	2.39	0.003
T. thermophilus Cu_A	0.84	1.96	0.004	2.29	0.011	2.43	0.002

[a] The coordination numbers in the simulations were fixed at 1.0 N, 2.0 S, and 1.0 Cu scatterers per Cu_A absorber. Distances are accurate to ±0.02 Å. Data for the mixed-valence Cu_A center of *T. thermophilus* are included for comparison.

MCD *C*-term intensities derived from out-of-state spin−orbit coupling between an excited state and the ground state deviate from the "sum rule" observed for pseudo-*A*-terms, and this behavior is evident in the remaining transitions in the purple Cu_A azurin MCD spectrum, as well as in the wild-type azurin MCD spectrum, where significantly more negative than positive MCD intensity is observed in the UV/vis/near-IR range measured. Therefore, MCD spectroscopy implicates significant out-of-state spin−orbit coupling of the ground state with low-lying excited states in each of these systems. Previous EPR analysis[42] of the Cu_A center in N_2OR also suggests the presence of significant spin−orbit coupling between the ground state and a low-lying excited state, and from these data this excited state is estimated to occur at ~3500 cm^{-1} above the ground state.

The similarity between the UV−vis absorption and MCD spectra of purple Cu_A azurin, shown in Figure 4a,b, and those of native Cu_A sites in both COX and N_2OR (Table 2)[45,46,98] argues strongly not only for their similar geometric structures, as demonstrated by the EXAFS data (*vide infra*), but also for very similar bonding characteristics and electronic structures. The differences, primarily in the specific energies and intensities of the observed transitions, therefore provide a useful link between geometric and electronic perturbations within the valence-delocalized $Cu_2(\mu\text{-Cys-}S)_2$ unit. In particular, the electronic transition responsible for the near-IR absorption maximum at 770 nm in purple Cu_A azurin has been assigned on the basis of previous resonance Raman studies of other Cu_A sites as involving a one-electron promotion between symmetric and antisymmetric dimer orbitals having significant Cu−Cu $\sigma \rightarrow \sigma^*$ character.[48,97] From Table 2, this absorption maximum is seen to occur at higher energy in purple Cu_A azurin than in the majority of other Cu_A sites, and this behavior may be correlated to the contraction of the $Cu_2(SR)_2$ core observed by EXAFS spectroscopy for this system (Table 3; *vide infra*), which would increase the splitting between the Cu−Cu σ and σ^* molecular orbitals. Further support for this observation has been provided by the study of Tolman's model complex, which has a Cu−Cu distance of 2.92 Å and a near-IR band of 1466 nm.[48,99] However, close comparison of the absorption and MCD spectra in this region[45,100] reveals the presence of a second, weaker absorption feature in the same energy region that is more apparent in the near-IR MCD spectrum of purple Cu_A azurin

(94) Peipho, S. B.; Schatz, P. N. *Group Theory in Spectroscopy*; Wiley-Interscience: New York, 1983.
(95) Rivoal, J. C.; Briat, B. *Mol. Phys.* **1974**, *27*, 1081−1108.
(96) Gerstman, B. S.; Brill, A. S. *J. Chem. Phys.* **1985**, *82*, 1212−1230.
(97) Wallace-Williams, S. E.; James, C. A.; de Vries, S.; Saraste, M.; Lappalainen, P.; van der Oost, J.; Fabian, M.; Palmer, G.; Woodruff, W. H. *J. Am. Chem. Soc.* **1996**, *118*, 3986−3987.
(98) Scott, R. A.; Zumft, W. G.; Coyle, C. L.; Dooley, D. M. *Proc. Natl. Acad. Sci. U.S.A.* **1989**, *86*, 4082−4086.
(99) Houser, R. P.; Young, V. G., Jr.; Tolman, W. B. *J. Am. Chem. Soc.* **1996**, *118*, 2101−2102.

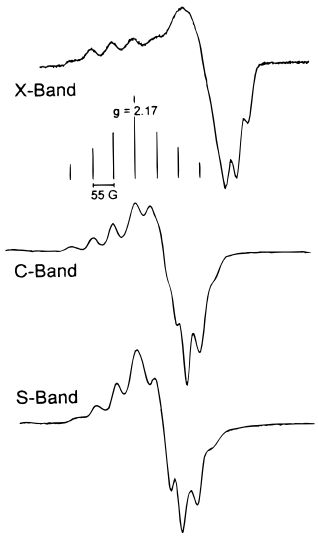

Figure 5. X-band (9.2 GHz), C-band (4.5 GHz), and S-band (3.4 GHz) EPR spectra aligned about $g_{||}$. Vertical lines mark the center of a seven-line pattern, i.e. $g_{||}$, and the seven-line pattern with relative intensities 1:2:3:4:3:2:1 for a single electron delocalized over two equivalent coppers. The concentration of purple Cu_A azurin was 0.8 mM.

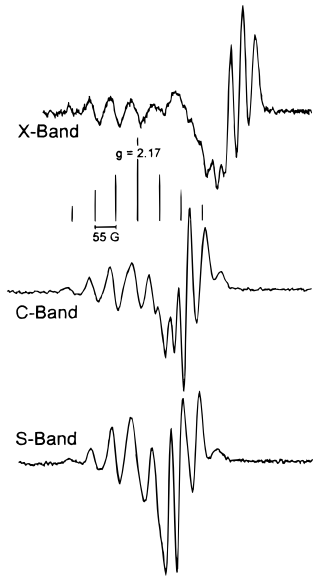

Figure 6. First harmonics of spectra in Figure 5 aligned along $g_{||}$.

than in the spectrum of *P. denitrificans*. Therefore, although the general trend between the near-IR Cu−Cu $\sigma \rightarrow \sigma^*$ absorption and the degree of $Cu_2(SR)_2$ core contraction is observed, quantitative correlation cannot be made until a careful deconvolution of the near-IR absorption bands and a firm assignment of the Cu−Cu $\sigma \rightarrow \sigma^*$ transition are accomplished. Further studies to clarify the spectroscopic properties of this and other Cu_A-type sites are in progress and will be reported in a separate publication.[100]

Multifrequency EPR. Multifrequency EPR spectra show well-resolved hyperfine structure in both the $g_{||}$ and $g_\perp$ regions (Figures 5 and 6). Five of the seven lines expected for a mixed-valence [Cu(1.5)···Cu(1.5)] $S = {}^1/_2$ delocalized center are apparent in the $g_{||}$ region of the X-band spectrum. While the $g_{||}$ and $g_\perp$ regions overlap more extensively at low frequencies,

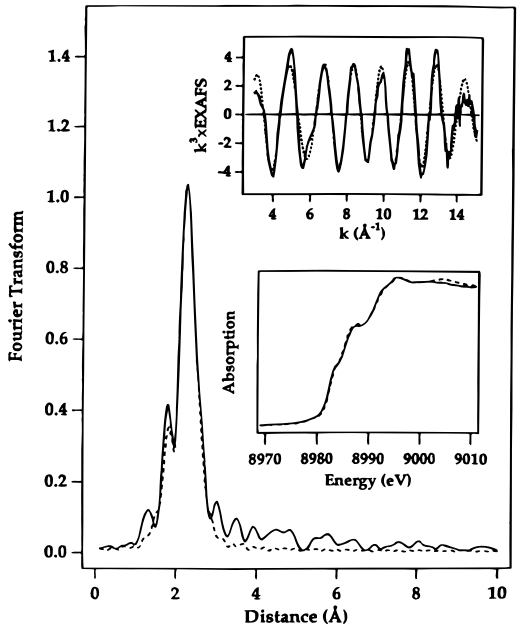

Figure 7. Experimental versus simulated Fourier transform and EXAFS (top inset) of the purple Cu_A azurin. Solid lines are experimental data, and dashed lines are simulated data. Bottom inset compares the Cu K absorption edges of purple Cu_A azurin (solid) and the *T. thermophilus* (dashed) Cu_A centers. The concentration of purple Cu_A azurin was 1.5 mM.

the center of the pattern at $g_{||} = 2.17$ confirms the existence of the seven-line pattern. The low frequency spectra are similar to spectra obtained for the mixed-valence [Cu(1.5)···Cu(1.5)] centers in COX and N_2OR.[18] One difference in the EPR parameters is that $A_{||}$ is 55 G in the purple Cu_A azurin spectrum, while $A_{||}$ is 38 G in COX and N_2OR. Also, the high-field lines are better resolved at 9.2 GHz than the high-field lines of the spectra for COX and N_2OR. Better resolution is consistent with good homogeneity of the sample and less *g*- and *A*-strain.

Multifrequency EPR spectra confirm the delocalized, mixed-valence, binuclear properties of the modified azurin site. Spectra from earlier studies[75] are not as well-resolved. Assuming the poor resolution is a result of sample heterogeneity, several possibilities exist. First, superposition of type 1 (blue) copper sites with the mixed-valence (purple) signal would result in poorer resolution of the hyperfine lines. Second, microwave power used in the earlier EPR study was unusually high. Third, a second mixed-valence signal could account for the poorer resolution. Such a signal has been uncovered in N_2OR and hypothesized to exist in COX.[101] Assuming a second mixed-valence signal accounts for the poor resolution in earlier samples requires a change in the EPR parameters for the second signal. Evidence for changes in the EPR parameters of the [His-*N*−Cu(1.5)−(*S*-Cys)$_2$−Cu(1.5)−*N*-His] center already exists. The copper hyperfine is decreased by about 20% from 38 to 30 G in cytochrome ba_3 from *T. thermophilus*,[28,43,44] and the copper hyperfine of the engineered Cu_A site in amicyanin from *T. versutus*[76] increased by about 30% to 50 G in a synthetic model complex[99] and about 50% to 55 G in this work.

XAS. The phase-corrected Fourier transform (FT) and EXAFS (inset) for purple Cu_A azurin is shown in Figure 7. The FT shows a single peak around $R = 2.4$ Å similar to that observed for the Cu_A sites of the soluble domain of *T. thermophilus* subunit II. Results presented in this paper, together

(100) Gamelin, D. R.; Randall, D. W.; Hay, M. T.; Houser, R. P.; Mulder, T. C.; Canters, G. W.; de Vries, S.; Tolman, W. B.; Lu, Y.; Solomon, E. I. *J. Am. Chem. Soc.*, submitted for publication.

(101) Antholine, W. E.; Kroneck, P. M. H.; Zumft, W. G. Manuscript in preparation.

with those reported previously,[75] have provided strong evidence for structural homology between the purple Cu_A azurin and the crystallographically characterized Cu_A center of COX[54−56] and the re-engineered quinol oxidase (CyoA).[57] We have therefore used the CyoA ligand atom donor set as the basis for our EXAFS analysis but have excluded the more distant methionine and main-chain carbonyl ligand atoms, as these did not contribute to the EXAFS data of either *T. thermophilus* or *B. subtilis*.[49] The best fit to the data was obtained with the parameters given in Table 3, *viz.* 1 Cu−N(His) at 1.92 Å, 2 Cu−S(cys) at 2.28 Å, and 1 Cu−Cu at 2.39 Å. The Cu−S(cys) distance is comparable to that found in *T. thermophilus*, but the Cu−N and Cu−Cu are 0.04 and 0.05 Å shorter, respectively. In fact, the Cu−Cu distance of 2.39 Å is the shortest distance yet determined for any of the Cu_A centers. This may reflect a more sterically compressed Cu_A center, perhaps as the result of forcing the normally mononuclear blue copper center in azurin to accept a binuclear Cu_A center, and is consistent with the MCD results (*vide supra*) which suggest a higher energy Cu−Cu interaction.

The inset to Figure 7 shows a comparison of the Cu K absorption edges of the oxidized azurin Cu_A and the *T. thermophilus* Cu_A derivatives. It is evident that the spectra superimpose exactly. This provides additional evidence that the geometric and electronic structures of the Cu_A centers in COX and in the azurin loop-directed mutant are very similar.

Conclusion

Copper centers in biological systems have been classified into three types.[31,32] The type 1, blue copper center is a mononuclear Cu(II)−thiolate center in a distorted tetrahedral geometry. The type 2, normal copper center has a mononuclear copper center in a tetragonal geometry. The type 3 copper center contains an anti-ferromagnetically coupled binuclear copper. The mixed-valent binuclear purple Cu_A center is a new class of copper centers. By engineering the purple Cu_A center into the type 1 copper protein azurin, we have shown the following:

1. The purple Cu_A center is structurally related to the type 1 blue copper center and it is possible to convert a blue copper center into a purple Cu_A center.

2. Loop-directed mutagenesis is a natural extension of site-directed mutagenesis and is a powerful way of engineering metal-binding sites in proteins.

3. The engineered purple Cu_A azurin presented here shows striking similarity to other native and engineered Cu_A centers, as evidenced by the UV−vis, MCD, multifrequency EPR, and XAS spectroscopic characterization presented in this paper, as well as by the RR study published earlier.[38]

4. When compared to the other delocalized mixed-valence Cu_A centers studied to date, the purple Cu_A azurin has one of the highest-energy near-IR Cu−Cu $\sigma \rightarrow \sigma^*$ absorption features at 770 nm, the largest $A_{\|}$ at 55 G, and the shortest Cu−Cu distance at 2.39 Å. These results may all relate to a higher degree of steric compression of the Cu_A center in azurin than in other Cu_A sites, which could perhaps occur as the result of forcing the normally mononuclear blue copper center in azurin to accept a binuclear Cu_A center.

Further study of this engineered purple Cu_A center in the same protein framework of the blue copper protein azurin, including electron transfer studies, is in progress and should contribute to our understanding of copper centers in biological systems.

Acknowledgment. We thank Professor John H. Richards at Caltech for providing the azurin gene, Professor John Shapley at the University of Illinois for the gift of $Cu(CH_3CN)_4BF_4$, Drs. Richard Milberg and Rong Huang at the University of Illinois Mass Spectrometry Center for collecting ES-MS spectra, Drs. Paige Goodlove and Nancy Lan-Fei Chang at the University of Illinois Genetic Engineering Facility for DNA sequencing and amino acid analyses, Dr. Louis B. LaCroix for providing the MCD spectrum of wild-type azurin from *P. aeruginosa*, Professor Hartmut Michel for providing crystallographic coordinates of cytochrome *c* oxidase from *P. denitrificans*, and Mr. Jeffrey A. Sigman for help in generating Figure 1. This material is based upon work supported by the National Science Foundation under Award Nos. CHE 95-02421 to Y.L. (CAREER Award) and CHE-9217628 to E.I.S. The multifrequency EPR work was supported by the National Institutes of Health under the Award No. RR01008 to W.E.A. The XAS work was supported by grants from the Murdock Charitable Trust and the National Institutes of Health (under Award No. GM52830) to N.J.B. We gratefully acknowledge the use of facilities at the Stanford Synchrotron Radiation Laboratory (SSRL), which is supported by the National Institutes of Health Biomedical Research Technology Program, Division of Research Resources, and by the Department of Energy, Office of Health and Environmental Research. Y.L. is a Beckman Young Investigator of the Arnold and Mabel Beckman Foundation and a Cottrell Scholar of the Research Corp.

IC971232A